Cascaded third-harmonic generation in a single short-range-ordered nonlinear photonic crystal

Yan Sheng,[1,*] Solomon M. Saltiel,[2] and Kaloian Koynov[1]

[1]*Max Planck Institute for Polymer Research, Ackermannweg 10, D-55128, Mainz, Germany*
[2]*Faculty of Physics, University of Sofia, 5 J. Bourchier Boulevard, 1164-Sofia, Bulgaria*
**Corresponding author: sheng@mpip-mainz.mpg.de*

Received November 6, 2008; revised December 22, 2008; accepted December 23, 2008;
posted January 22, 2009 (Doc. ID 103778); published February 25, 2009

Collinear third-harmonic generation at 526.7 nm was realized by the simultaneous phase matching of two second-order processes in a single quadratic crystal: second-harmonic generation (SHG) and sum-frequency mixing (SFM). The measured conversion efficiency was 12%. As a nonlinear medium a $LiNbO_3$ nonlinear photonic crystal with short-range order was used that allowed simultaneous phase matching by use of discrete reciprocal vector (for the SHG process) and continuous reciprocal vectors (for the SFM process). It was demonstrated that the third harmonic could be generated efficiently in such a crystal even if the intermediate process of SHG was not perfectly phase matched.

OCIS codes: 190.0190, 190.2620, 190.4410, 220.4000, 230.1150.

Recent advances in quasi-phase-matching (QPM) technology based on nonlinear photonic crystals (NPCs) with modulated quadratic nonlinear susceptibility [or $\chi^{(2)}$] have motivated great interest in the physics and applications of multistep optical parametric processes [1]. In particular, the frequency converters for the third-harmonic generation (THG) in a single NPC, in which two parametric processes of second-harmonic generation (SHG) $\omega+\omega=2\omega$ and sum-frequency mixing (SFM) $\omega+2\omega=3\omega$ are simultaneously phase matched, have been studied extensively. A great part of these works were done in one-dimensional (1D) NPCs [2–6], and THG efficiency about 20% was achieved [2]. Since Berger pointed out fascinating properties of QPM in two-dimensional (2D) structures for SHG [7], extensions of their use for THG have been made [8–12]. However, the periodic 2D NPCs that have been experimentally investigated so far lead to noncollinear THG, which sometimes limits their practical use. In addition, the design of periodic 2D NPCs for THG requires extremely accurate knowledge of crystal index refraction in a broad spectral range (λ–3λ) that usually is not available with the existing data. A slight change of temperature or angular position cannot help, since adjustment of one of the interactions to the exact phase-matching point leads to serious deviation from the phase-matching point for the second interaction.

Recently, we proposed and demonstrated a short-range-ordered (SRO) 2D NPC, whose $\chi^{(2)}$ tiling was controlled by a random function and structural long-range order was broken [13]. Such a 2D NPC can provide continuous reciprocal vectors (RVs) in the shape of concentric rings, thus allowing us to achieve phase matching of any second-order process over a broad range of wavelengths, and is insensitive to temperature or angular position [13,14]. In this Letter we demonstrate how to exploit the unique properties of such an NPC to realize a collinear THG in a single crystal. Taking advantage of the continuous RVs, we were able to show that the third harmonic can be generated efficiently even when the intermediate process of SHG is suffering a certain phase mismatch. Furthermore, as the ratio of the RVs can be adjusted freely by proper design of the NPC, cascaded THG can be achieved at any given wavelength in the transparency range of the crystal.

The SRO NPCs were fabricated using electric-field poling of a z-cut $LiNbO_3$ wafer [15,16]. The domain-inverted structure is shown in Fig. 1(a), where the inset illustrates how the SRO structure is created by placing randomly rotated basic units on a square lattice of period $b=19.8$ μm. The basic units themselves are also squares with a side length of $a=8.5$ μm. The length of the poled sample was 12 mm.

Figure 1(b) shows the diffraction pattern of the SRO NPC oriented with its z axis parallel to the incident He–Ne laser beam. The locations of the diffractive spots correspond to the RVs available for QPM. There are two kinds of RVs: discrete RVs ($\mathbf{G_{m,n}}$) arranged into a square lattice and continuous RVs ($\mathbf{G_c}$) in the shape of concentric rings. We have explored the origin of such diffraction patterns in earlier works [13,14], showing that $\mathbf{G_{m,n}}$ and $\mathbf{G_c}$ are completely independent of each other. In fact, $\mathbf{G_{m,n}}$

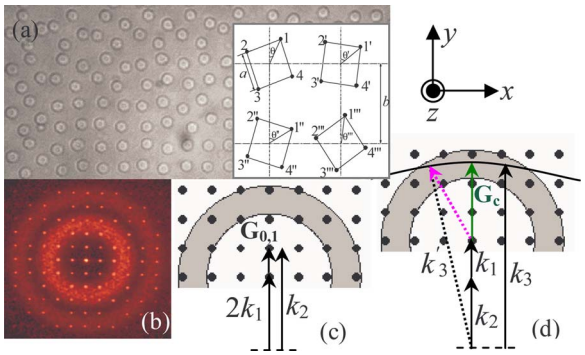

Fig. 1. (Color online) (a) Domain structure of an SRO NPC, where the inset illustrates how it is created. (b) Diffraction pattern. (c) and (d) QPM diagrams for SHG using $\mathbf{G}_{0,1}$ and SFM using $\mathbf{G_c}$. The dotted lines illustrate the striplike TH caused by noncollinear interactions contributing in the wings.

are RVs that correspond to the main square lattice and are defined by the two basic vectors $|\mathbf{G}_{0,1}| = |\mathbf{G}_{1,0}| = 2\pi/b$; $\mathbf{G}_c$ comes from the random rotations of the basic units and depends only on a. To realize double-phase-matched THG, joint actions of such discrete and continuous RVs should be used: achieve SHG through $\mathbf{G}_{0,1}$ and then realize SFM through suitable $\mathbf{G}_c$, as schematically shown in Figs. 1(c) and 1(d), respectively. For the SRO NPC, the QPM conditions for collinear THG are $\Delta k_1 = k_2 - 2k_1 = |\mathbf{G}_{0,1}|$ for SHG and $\Delta k_2 = k_3 - k_2 - k_1 = |\mathbf{G}_c|$ for SFM, where k_1, k_2, and k_3 are the wave vectors of the fundamental, second-, and third-harmonic (SH and TH) fields, respectively. Using these relations, a simple two-step procedure may be derived for the design of an SRO NPC allowing cascaded THG at a given wavelength. First, the lattice constant b should be determined using $b = 2\pi/\Delta k_1$. Second, a value of a that will locate Δk_2 inside one of the concentric rings of RVs (see Fig. 2) should be chosen using the set of analytical equations presented in [14]. The usage of $\mathbf{G}_c$ in the first ring is recommended for higher conversion efficiency. As the RV rings are fairly broad, slight changes of temperature or angular position of the crystal can be used to optimize the SHG process without compromising the SFM phase matching. Furthermore, each of the two steps can be phase matched by adjusting different parameters of the NPC (b and a). Thus their ratio and magnitude can be tuned freely so that simultaneous phase matching of any two required processes can be achieved. This is a significant advantage of the SRO NPC in comparison with other schemes for cascaded high-order harmonic generation in a single crystal. In the particular case of cascaded THG this makes QPM possible at an arbitrary fundamental wavelength.

To demonstrate the efficiency of the above-described procedure and achieve cascaded THG at 526.7 nm, we have designed the NPC shown in Fig. 1(a). The Sellmeier equation for a bulk $LiNbO_3$ at 25 °C was used to estimate the wavelength dependence of the refractive index [17]. As a light source we used an optical parametric generator–amplifier delivering a beam of 16 ps pulses with a repetition rate of 10 Hz. The input beam was focused, and the waist diameter at the input facet of the sample was about 100 μm. When the input wavelength was tuned to 1580.0 nm, a strong green light was observed on a white screen behind the sample. The spectrum was analyzed by a fiber spectrometer. As shown in Fig. 2(a) two peaks at 790.0 nm and at 526.7 nm, corresponding to the SH and TH, are clearly observed. The SH and TH beams were centered in the position of the fundamental beam. Figures 2(b) and 2(c) show the spatial distributions of their intensities, respectively. While the SH spot is circular, the TH beam has a striplike form caused by noncollinear interactions contributing in the wings [see Fig. 1(d)].

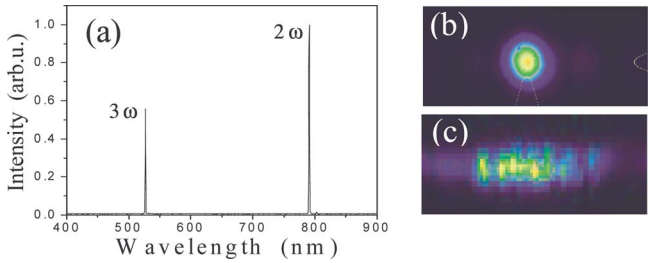

Fig. 2. (Color online) (a) Spectrum measured at the output end of the sample; (b) SH and (c) TH beam profiles.

Figure 3 shows the wavelength-tuning curves of the NPC, i.e., the harmonic pulse energies, versus the fundamental wavelength, with a constant input pulse energy of 1.73 μJ. It is seen that TH energy reaches its maximum at 1580.0 nm, where we believe the double-QPM conditions are satisfied. When we detune the wavelength, the harmonic energies decline rapidly. The SH drops, because its phase mismatch (Δk_1) increases with the wavelength detuning. The THG depends on the intermediate SH energy, so it falls, too. It is worth noting that the SFM process, which is governed by the continuous RVs, remains phase matched within such a wavelength detuning. Therefore, the observed THG detuning curve is quite different from the earlier reported schemes [2–4,8–12] in which SFM contributes as much as SHG does to the drop of TH energy.

Figure 4(a) shows the harmonic energies against input energy at 1580.0 nm wavelength. The same measurements are displayed in Fig. 4(b), but the fundamental wavelength is 1584.0 nm, i.e., deviating 4.0 nm from the optimal, and therefore SHG is phase mismatched. The corresponding conversion efficiencies are shown in Figs. 4(c) and 4(d), respectively. Theory predicts that the SH (TH) conversion efficiency increases linearly (quadratically) with input energy at a low excitation limit [2]. Such behavior is present in Fig. 4(c) at an input energy of less than 0.5 and 2.2 μJ, respectively. The normalized SH and TH conversion efficiencies calculated with respect to a single pulse power in this nondepleted pump region are $2.0 \times 10^{-3}\%$ W^{-1} and $0.64 \times 10^{-9}\%$ W^{-2}, respectively. These values can be compared with those reported recently for a noncollinear scheme in a 1D periodic structure [6]: $2.3 \times 10^{-3}\%$ W^{-1} for SH and $4.4 \times 10^{-8}\%$ W^{-2} for TH. The agreement for SH is good. The lower efficiency for THG can be explained by the lower value of $d_{\mathrm{eff}}^{(2)}$ for the mixing process and by the role of the group-velocity mismatch.

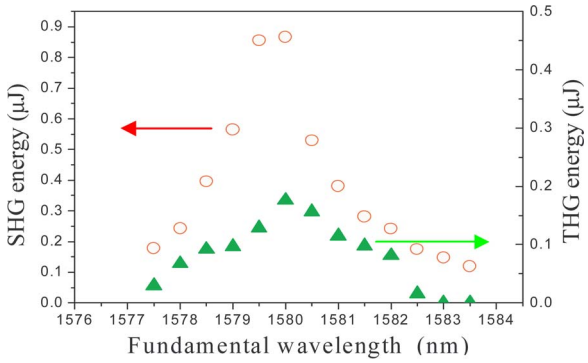

Fig. 3. (Color online) Wavelength-tuning curves obtained with the simultaneous recording of both harmonics.

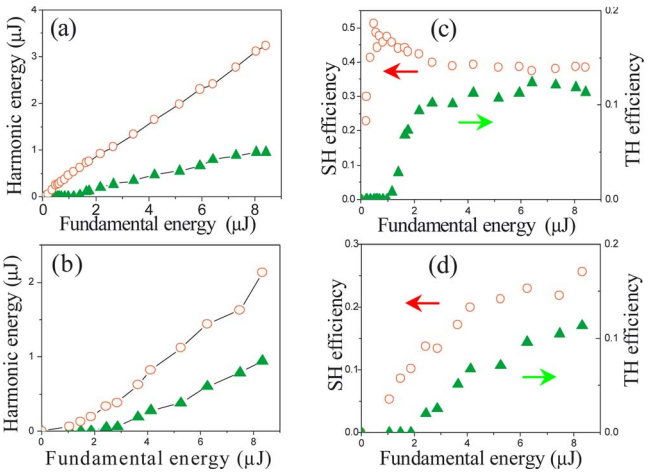

Fig. 4. (Color online) SH (dots) and TH (triangles) energies and efficiencies versus. input energy at (a) and (c) double QPM of 1580.0 nm, and (b) and (d) 1584.0 nm.

When input energy goes higher, the efficiency of SHG first drops, because more and more energy is converting to TH, and afterwards it saturates at 40% owing to the backconversion effect [15]. At these fundamental energy levels the THG efficiency saturates at ~12%. When the fundamental wavelength was tuned to 1584.0 nm, the SHG was phase mismatched. As a result, the saturation occurred at a higher energy level with a lower efficiency: 25% at 4.2 μJ input [Fig. 4(d)]. The maximal efficiency of THG, however, can still reach 12%, the same value as in the double-QPM case. This means that the efficient THG is observed even when the intermediate SHG process is suffering a certain phase mismatch, a finding that agrees well with theoretical predictions [2,18]. Of course, the significance of a phase-matched SHG should not be underestimated. Since at input energies below the saturation level the efficiency of THG depends strongly on the SH energy; the smaller the SHG mismatch is, the higher THG efficiency can be achieved. For example with an input energy of 2.2 μJ, the THG efficiency reaches 10% in the double-QPM condition, whereas only 2% if SHG is not phase matched [Figs. 4(c) and 4(d)].

In conclusion, we have designed and fabricated a $LiNbO_3$ NPC with short-range order and have realized cascaded THG at 526.7 nm with an efficiency about 12%. It has been experimentally demonstrated that the efficient THG could be realized in such an NPC even if the intermediate process of SHG is not perfectly phase matched. The proposed scheme for the phase matching of two nonlinear processes in an SRO NPC makes cascaded THG at any given wavelength possible. The same approach can be used for fourth-harmonic generation in a single crystal.

The joint financial support of Max Planck Society, Chinese Academy of Sciences (CAS), and Deutscher Akademischer Austauschdienst is gratefully acknowledged.

References

1. S. M. Saltiel, A. A. Sukhorukov, and Y. S. Kivshar, Prog. Opt. **47**, 1 (2005).
2. S. Zhu, Y. Zhu, and N. Ming, Science **278**, 843 (1997).
3. O. Pfister, J. S. Wells, L. Hollberg, L. Zink, D. A. Van Baak, M. D. Levenson, and W. R. Bosenberg, Opt. Lett. **22**, 1211 (1997).
4. K. Fradkin-Kashi, A. Arie, P. Urenski, and G. Rosenman, Phys. Rev. Lett. **88**, 023903 (2002).
5. R. Ivanov, K. Koynov, and S. Saltiel, Opt. Commun. **212**, 397 (2002).
6. T. Ellenbogen, A. Arie, and S. M. Saltiel, Opt. Lett. **32**, 262 (2007).
7. V. Berger, Phys. Rev. Lett. **81**, 4136 (1998).
8. N. G. R. Broderick, R. T. Bratfalean, T. M. Monro, D. J. Richardson, and C. M. de Sterke, J. Opt. Soc. Am. B **19**, 2263 (2002).
9. S. Saltiel and Y. S. Kivshar, Opt. Lett. **25**, 1204 (2000).
10. B. Ma, T. Wang, P. Ni, B. Cheng, and D. Zhang, Europhys. Lett. **68**, 804 (2004).
11. K. Fradkin-Kashi, A. Arie, P. Urenski, and G. Rosenman, Phys. Rev. Lett. **95**, 133901 (2005).
12. N. Fujioka, S. Ashihara, H. Ono, T. Shimura, and K. Kuroda, J. Opt. Soc. Am. B **24**, 2394 (2007).
13. Y. Sheng, J. Dou, B. Ma, B. Cheng, and D. Zhang, Appl. Phys. Lett. **91**, 011101 (2007).
14. Y. Sheng, J. Dou, J. Li, B. Cheng, and D. Zhang, Appl. Phys. Lett. **91**, 101109 (2007).
15. P. Ni, B. Ma, X. Wang, B. Cheng, and D. Zhang, Appl. Phys. Lett. **82**, 4230 (2003).
16. Y. Sheng, T. Wang, B. Ma, B. Cheng, and D. Zhang, Appl. Phys. Lett. **88**, 041121 (2006).
17. D. H. Jundt, Opt. Lett. **22**, 1553 (1997).
18. S. Longhi, Opt. Lett. **32**, 1791 (2007).